Ecotoxicology and Environmental Safety 264 (2023) 115468

Contents lists available at ScienceDirect

Ecotoxicology and Environmental Safety

journal homepage: www.elsevier.com/locate/ecoenv

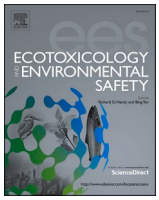

Elucidating the spatial distribution of organic contaminants and their biotransformation products in amphipod tissue by MALDI- and DESI-MS-imaging

Johannes Raths [a,b,1], Fernanda E. Pinto [c,2], Christian Janfelt [c,3], Juliane Hollender [a,b,*,4]

[a] Department of Environmental Chemistry, Swiss Federal Institute of Aquatic Science and Technology - Eawag, Dübendorf, Switzerland
[b] Institute of Biogeochemistry and Pollutant Dynamics, ETH Zürich, Zürich, Switzerland
[c] Department of Pharmacy, University of Copenhagen, Copenhagen, Denmark

ARTICLE INFO

Edited by Dr G Liu

Keywords:
Aquatic invertebrates
Bioaccumulation
Cryosectioning
Dissection
Gammarus pulex
Micropollutants
Whole body cross sections

ABSTRACT

The application of mass spectrometry imaging (MSI) is a promising tool to analyze the spatial distribution of organic contaminants in organisms and thereby improve the understanding of toxicokinetic and toxicodynamic processes. MSI is a common method in medical research but has been rarely applied in environmental science. In the present study, the suitability of MSI to assess the spatial distribution of organic contaminants and their biotransformation products (BTPs) in the aquatic invertebrate key species *Gammarus pulex* was studied. Gammarids were exposed to a mixture of common organic contaminants (carbamazepine, citalopram, cyprodinil, efavirenz, fluopyram and terbutryn). The distribution of the parent compounds and their BTPs in the organisms was analyzed by two MSI methods (MALDI- and DESI-HRMSI) after cryo-sectioning, and by LC-HRMS/MS after dissection into different organ compartments. The spatial distribution of contaminats in gammarid tissue could be successfully analyzed by the different analytical methods. The intestinal system was identified as the main site of biotransformation, possibly due to the presence of biotransforming enzymes. LC-HRMS/MS was more sensitive and provided higher confidence in BTP identification due to chromatographic separation and MS/MS. DESI was found to be the more sensitive MSI method for the analyzed contaminants, whereas additional biomarkers were found using MALDI. The results demonstrate the suitability of MSI for investigations on the spatial distribution of accumulated organic contaminants. However, both MSI methods required high exposure concentrations. Further improvements of ionization methods would be needed to address environmentally relevant concentrations.

1. Introduction

Aquatic invertebrates play a critical role in the functioning of aquatic ecosystems, and their health is often an indicator of environmental quality (Chaumot et al., 2015). Such organisms are susceptible towards environmental contaminants, which are mostly released by anthropogenic activities (Wang et al., 2020). Environmental contaminants can be taken up by aquatic invertebrates from the water directly (bioconcentration) or from contaminated diet (biomagnification) (OECD, 2012; Schlechtriem et al., 2019). Toxicokinetics describe all processes that determine the internal body burden, such as uptake, internal distribution, biotransformation and elimination. Internal concentrations, or more specifically the concentrations at the target site, determine subsequent toxicological effects, which can cause a range of negative impacts on the physiology and behavior of aquatic invertebrates, ultimately affecting their survival and reproductive success (Escher and Hermens, 2002). Furthermore, biotransformation is an important modulator of xenobiotic toxicity by mostly increasing detoxification (deactivation) kinetics (Ashauer et al., 2012; Rösch et al., 2017), but also leading to the toxicological activation of some compounds (Fu et al., 2020). Biotransformation enzymes, such as cytochrome monooxygenases (i.e., CYP 450), are expressed in different

* Corresponding author at: Department of Environmental Chemistry, Swiss Federal Institute of Aquatic Science and Technology - Eawag, Dübendorf, Switzerland.
E-mail address: juliane.hollender@eawag.ch (J. Hollender).
[1] **Orchid ID:** https://orcid.org/0000-0002-3258-0893.
[2] **Orchid ID:** https://orcid.org/0000-0002-2300-8481.
[3] **Orchid ID:** https://orcid.org/0000-0002-4626-3426.
[4] **Orchid ID:** https://orcid.org/0000-0002-4660-274X.

https://doi.org/10.1016/j.ecoenv.2023.115468
Received 6 July 2023; Received in revised form 29 August 2023; Accepted 8 September 2023

intensities across various organs, with organs such as the liver of vertebrates or hepatopancreas of arthropods being the main sites of biotransformation (James, 1989). Thus, the ability to determine the spatial distribution of contaminants and biotransformation sites in an organism is important for understanding toxic effects.

Conventional sample workup for tissue residue analysis in aquatic invertebrates includes whole sample homogenization (Munz et al., 2018) and thereby all spatial information is lost. The separate analysis of dissected compartments is commonly applied for vertebrates, such as fish (Davis et al., 2020; Grabicova et al., 2014; Schultz et al., 2010; Zeumer et al., 2020), but for smaller invertebrates this method can be very time-consuming, requires specific skills (Gestin et al., 2022, 2021; Kampe and Schlechtriem, 2016) or is even not feasible (i.e. the exoskeleton and muscle or ventral nerve of amphipods cannot be separated; Miller et al., 2016; Rubach et al., 2010). The application of imaging approaches represents a promising alternative but experiences with aquatic invertebrates are so far limited to methods like radio imaging which uses organisms exposed to radiolabeled contaminants (Arts et al., 1995; Nyman et al., 2014; Raths et al., 2020). Radio imaging facilitates a high sensitivity by using relatively simple analytical instrumentation. However, one significant drawback of radio imaging is that it does not allow a discrimination between a parent compound and its biotransformation products (BTPs) or even mineralized compound (i.e., ^{14}C incorporated into calcium carbonate of the exoskeleton of amphipods; Raths et al., 2020), which may cause various analytical artefacts. An alternative approach that avoids such drawbacks is the analysis by mass spectrometry imaging (MSI). MSI is an intensively applied method in medical sciences (Chughtai and Heeren, 2010; Dong et al., 2016) but gained attention in environmental sciences only recently (Maloof et al., 2020; Yang et al., 2020). The use of high-resolution mass spectrometry (HRMS) in MSI, allows to locate and discriminate multiple small organic compounds within the same sample, including various organic contaminants and their BTPs.

Two commonly applied ionization techniques in MSI are matrix assisted laser desorption ionization (MALDI) and desorption electrospray ionization (DESI), which are able to detect a wide range of analytes including small organic molecules (i.e., pesticides and pharmaceuticals), their transformation products, neurotransmitters, lipids, peptides, and proteins (Chughtai and Heeren, 2010; Dong et al., 2016). Both techniques are soft ionization methods (low in-source fragmentation) that can be performed at atmospheric pressure and be connected to a variety of mass spectrometer instrumentations including high resolution mass spectrometers (Maloof et al., 2020). Whereas MALDI generally allows a smaller spatial resolution (e.g. down to the 5–20 μm range) which may be desired for the analysis of aquatic invertebrates, DESI may be the more sensitive technique for small organic molecules but at a cost of spatial resolution (e.g. 50–200 μm range). Furthermore, DESI requires less sample preparation such as matrix application, and apart from saving resources, may result in reduced artefacts introduced by background masses compared to such that may be introduced by MALDI-matrices. To our knowledge, a direct comparison of the two methods has not been done yet.

The goal of the study was to determine the suitability of MSI to assess the spatial distribution of organic contaminants and their BTPs in the aquatic invertebrate key species *Gammarus pulex* (Linnaeus, 1758). Therefore, the spatial distribution within exposed gammarids is analyzed by two MSI methods (MALDI and DESI). For comparison, the organisms were also dissected and individual parts analyzed with LC-HRMS/MS. We hypothesized that (I) MSI supports the spatial elucidation of organic contaminants in aquatic invertebrates and that (II) BTPs follow a distinct distribution within the organism, depending on their site of biotransformation (i.e., the hepatopancreas).

2. Material and methods

2.1. Test animals

Specimens of *G. pulex* were collected from an uncontaminated creek near Zurich (Mönchaltdorfer Aa, 47.2749°N, 8.7892°E), located in a landscape conservation area. Genetic specifications of the population are reported elsewhere (Raths et al., 2023c). All animals used in the performed experiments were acclimated to the test conditions for four days prior to the experiments and fed with leaf material collected in the field. Artificial pond water (Naylor et al., 1989) was used as a laboratory medium and permanently aerated. The temperature was 16 ± 1 °C and the light condition 12:12 h (light:dark). Only male gammarids – separated based on the presence of large secondary gnathopods (Hume et al., 2005) – with a size of > 8 mm were used in order to obtain a sufficient size for imaging and dissection. Gammarids with visible parasitism (i.e. acanthocephalans; Kochmann et al., 2023) were excluded as these may influence the distribution of contaminants in the organism.

2.2. Test compounds and exposure

The selected exposure mixture contained six organic contaminants commonly found in surface water monitoring studies (Lauper et al., 2021; Munz et al., 2018) of which three were pharmaceuticals (carbamazepine, citalopram, efavirenz), two fungicides (cyprodinil, fluopyram) and one herbicide (terbutryn). An overview of the tested compounds, including the applied exposure concentration, log D_{ow} (octanol-water partitioning coefficient to account for speciation at pH 7.9) and references for biotransformation products are provided in Table 1. Due to the necessary high exposure concentrations, toxicity of the compounds had to be considered and several other exposure-relevant compounds could not be included.

The test basin (6 L) was spiked with the exposure mixture (Table 1) dissolved in < 3 mL methanol. After 30 min, gammarids were inserted (16 specimens L^{-1}) and exposed for 24 h. Additionally, control gammarids were treated similarly, but without contaminants in the medium.

Gammarids used for MSI and total tissue concentration analysis were collected, rinsed with nanopure water (arium® pro, Sartorius AG), dry blotted on tissue paper, transferred into 2 mL centrifuge vials, weighed (wet weight (*ww*)) and frozen in liquid nitrogen. An experimentally determined conversion factor of 5.4 between wet and dry weight can be applied (Raths et al., 2023b).

For the determination of tissue specific concentrations, gammarids were tranquilized on ice and dissected (Fig. 1A) into cephalon (head),

Table 1
Compounds selected for the exposure mixture. Exposure = exposure concentration in the test basin. Log D_{ow} values are obtained from https://pubchem.ncbi.nlm.nih.gov/. BTP = biotransformation product. An extension of this table, including the corresponding toxicity values is provided in Table S1.

Compound	Molecular formula	Exposure [mg L^{-1}]	log D_{ow} (main species)	BTP references
Carbamazepine	$C_{15}H_{12}N_2O$	2.2	2.3 (neutral)	(Jeon and Hollender, 2019)
Citalopram	$C_{20}H_{21}FN_2O$	0.8	1.9 (cation)	(Raths et al., 2023c; Sangkuhl et al., 2011)
Cyprodinil	$C_{14}H_{15}N_3$	0.35	4.0 (neutral)	(Kiefer et al., 2019; Raths et al., 2023c; Sapp et al., 2004)
Efavirenz	$C_{14}H_9ClF_3NO_2$	0.10	4.6 (neutral)	(Mutlib et al., 2000)
Fluopyram	$C_{16}H_{11}ClF_6N_2O$	0.50	3.3 (neutral)	(Vargas-Pérez et al., 2020)
Terbutryn	$C_{10}H_{19}N_5S$	1.00	3.7 (neutral)	(Jeon et al., 2013)

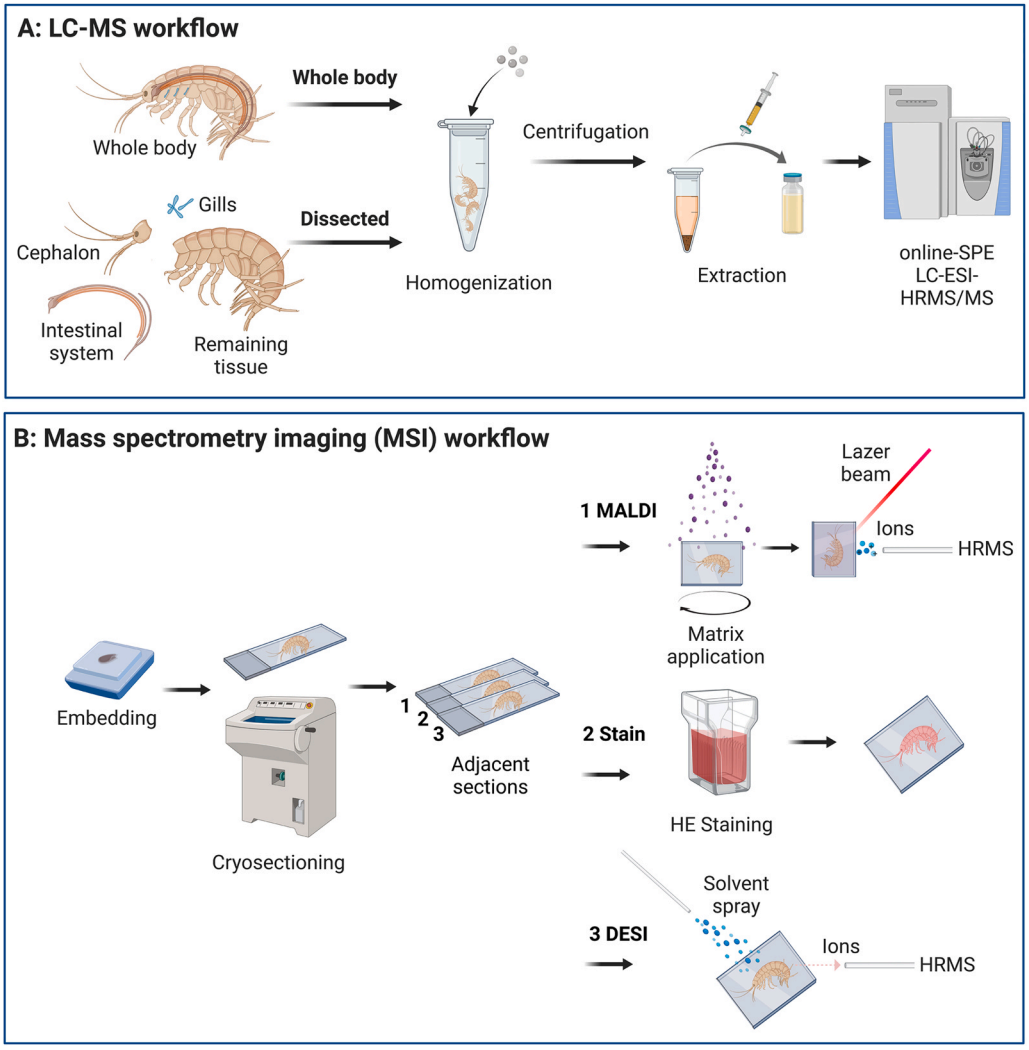

Fig. 1. (A) The workflow of dissection, tissue extraction and extract analysis by online-SPE LC-HRMS/MS. Replicates of gammarids were analyzed either as a whole for the determination of the whole body concentration ("conventional method") or dissected into cephalon, intestinal system, gills and remaining tissue. (B) The workflow for cryosectioning and MSI analysis. Three adjacent cross-sections were created and analyzed by either MALDI-HRMSI (1), histological staining (2) or DESI-HRMSI (3).

intestinal system (hepatopancreas (caeca/midgut) and intestine (foregut and hindgut)), gills, and remaining tissue based on the methods provided by Gestin et al. (2022). The dissected compartments of three gammarids were pooled into 2 mL centrifuge vials, weighed (*ww*) and frozen in liquid nitrogen. All samples were stored at − 80 °C until further analysis.

2.3. Sample extraction

Samples collected for tissue concentration determination were extracted by liquid extraction as described elsewhere (Rösch et al., 2016). In brief, 300 mg of 1 mm zirconia/silica beads (BioSpec Products, Inc.), 100 μL of isotope labeled internal standard mixture (250 μg L^{-1} deuterated reference standards, Table S6) in methanol and 500 μL of pure methanol were added before samples were homogenized using a FastPrep bead beater (two cycles of 15 s at 6 m s^{-1}; MP Biomedicals). Samples were then centrifuged (10,000 × *g*, 6 min, 4 °C). Afterwards, the solvent was collected with syringes and filtered through 0.45 μm regenerated cellulose filters. The filters were washed with another 400 μL of pure methanol and the two filtrates combined.

Medium samples (100 μL) were collected at the beginning and the end of the exposure time, spiked with 100 μL of internal standard mixture in methanol and mixed with another 800 μL of pure methanol. All samples were stored at − 20 °C until chemical analysis.

2.4. LC-HRMS/MS analysis

The analysis of extract concentrations was performed using an automated online solid phase extraction system coupled with a reversed phase liquid chromatography column and high-resolution tandem mass spectrometer (online-SPE-LC-HRMS/MS; QExactive Plus, Thermo Fisher Scientific Inc.) using an electrospray ionization interface for ionization. The full scan acquisition was performed with a resolution of 70,000 (at *m/z* 200) in positive ion mode followed by data dependent MS/MS scans with a resolution of 17,500 (at *m/z* 200) and an isolation window of 1 *m/z*. Acquired HRMS/MS data were evaluated using the TraceFinder 5.1 software (Thermo Fisher Scientific Inc.). Detailed information on the test system, quality control and quantification are provided in SI A2.

For BTP identification, a suspect screening was performed, based on previously identified and reported BTPs in amphipods or other organisms and reference standards available in house (Table S7). Exact masses of molecular ions of BTPs were screened by using the acquired HRMS/MS raw data requiring their unique presence in the treatment and absence in all controls. BTPs were confirmed using their fragmentation patterns or if available, reference standards. If possible, BTPs were quantified using a reference standard. Other BTPs were semi-quantified based on the calibration curve of the parent compound. BTPs of terbutryn were semi-quantified based on the calibration of TER_M214, due to a similar retention time and the higher ionization efficiency of the BTPs (Jeon et al., 2013; Raths et al., 2023c). Quantification was only performed for compounds with a concentration ≥ 5 % of the parent

compound after 24 h of exposure in any compartment (Table S7).

2.5. Preparation of cryosections

The creation of reproducible intact whole body cross sections of small organisms such as arthropods is challenging (Yang et al., 2020). Difficulties are caused by heterogeneous tissue types of arthropods (i.e., hard and fragile cuticle or exoskeleton, very soft internal tissue, and hemolymph) and extremities that cause air bubbles at the embedded sample. However, these challenges have been overcome by the adjustment of embedding media (Ohtsu et al., 2018; Strohalm et al., 2011), removal of extremities (i.e., legs and wings; Zhang et al., 2021) or the application of cryotape (Kawamoto and Kawamoto, 2021). The latter has been applied in the present study.

Gammarid samples for MSI were embedded in a mounting medium of 2.5 % of carboxymethyl-cellulose (CMC). Embedding was performed using a steel cryomould submerged into a − 80 °C precooled n-hexane/dry ice bath (Kawamoto and Kawamoto, 2021). To reduce potential thawing, and thus delocalization, the cryomould was first submerged until the edges of the embedding media started to freeze. Then, the gammarid sample was placed in the embedding media and submerged completely until frozen. Embedded samples were stored at − 80 °C until cryosectioning.

Cryosectioning was performed on a Leica CM3050S cryo-microtome (Leica Microsystems) at − 16 °C. The sectioning was assisted by using an adhesive cryo-film (Cryotape 2C(9), SECTION-LAB Co. Ltd.; Kawamoto and Kawamoto, 2021) in order to obtain multiple reproducible 16 μm thick full body sections of the fragile samples. The sections were then attached to a standard microscope slide using a double-sided adhesive carbon tape (Electron Microscopy Sciences) and again stored at − 80 °C until further use. Sagittal cross sections from the center of the gammarid sample were created in sets of three subsequent cross sections (Fig. 1B), which were later used for MALDI-MSI (1), histological staining (2) and DESI-MSI (3).

Cross sections adjacent to the imaged samples (2) were stained by hematoxylin and eosin staining (HE staining) using an adapted protocol from the Institute for Agricultural Sciences, Animal physiology, ETH Zürich (SI A4). Hematoxylin is an at low pH positively charged dye and stains negatively charged, basophilic, tissue components such as nucleic acids or acid proteoglycans blue. The subsequent applied eosin is a negatively charged dye that dyes acidophilic components, such as proteins of the cytoplasm bright red (Mulisch and Welsch, 2015).

2.6. Mass spectrometry imaging

Prior to MSI analysis, samples were dried by vacuum desiccation (5–10 min). Sample integrity and quality were evaluated under a light-microscope (Olympus BH-2 microscope, Olympus Corporation) at 400 × magnification using reflected light.

In preparation for MALDI-MSI, a matrix solution of 30 mg mL^{-1} 2,5-dihydroxybenzoic acid (DHB, Merck) in MeOH:H_2O (90:10) containing 1 % trifluoroacetic acid (TFA; to improve ionization efficiency) was applied using an in-house built (University of Copenhagen) pneumatic matrix sprayer. The application volume was 300 μL, applied at a flow rate of 30 μL min^{-1} (N_2 nebulizer gas pressure was 2 bar) from a distance of 100 mm while the sample was rotating at 600 rpm. Matrix crystals were evaluated for size and homogeneity under the light-microscope.

The MALDI-MSI experiments were performed at ambient conditions using an AP-SMALDI5 ion source (TransMIT GmbH) coupled with a QExactive Orbitrap high-resolution mass spectrometer (Thermo Scientific). The scans were performed in positive ion mode with a mass resolving power of 140,000 at *m/z* 200, a mass range of *m/z* 140–980 and a scan speed of 1 pixel s^{-1} in pixel mode. DHB matrix peaks at *m/z* 295.02131 $[2M + Na - 2\ H_2O]^+$ and 401.07440 $[5M + NH_4 - 4\ H_2O]^+$ were used as lock masses for internal mass calibration, ensuring a mass accuracy of 2 ppm or better.

The DESI-MSI experiments were performed using custom built DESI ion source (Thunig et al., 2011) coupled with a QExactive Orbitrap high-resolution mass spectrometer (Thermo Scientific). The spray solvent of MeOH:H_2O (90:10) containing 2 % formic acid (to improve ionization efficiency) was delivered at a flow rate of 3 μL min^{-1}. The orientation of the ion source was optimized prior to the analysis on a different sample cross section of the same organism. The scans were performed in positive ion mode with a mass resolving power of 140,000 at *m/z* 200, a mass range of *m/z* 100–1050.

The pixel size in all MSI experiments was set to 60 μm. Three biological replicates of adjacent sagittal cross sections were analyzed for the treatment and control samples, respectively, using either MSI approach.

2.7. Data analysis

The mass spectra obtained from the MSI experiments were converted into imzML files (Schramm et al., 2012) using the "RAW + UDP to IMZML" software (v1.6R170; TransMIT) before being analyzed in the MATLAB (MathWorks) based open source software MSiReader v1.02 (Bokhart et al., 2018; Robichaud et al., 2013). The *m/z* tolerance was set to ± 5 ppm. All MSI data were normalized to the total ion current (TIC). Reconstructed images of the *m/z* value of the protonated target compounds $[M + H]^+$ as well as their BTPs and (lipid) biomarkers (Table 2) were created as heatmaps and compared to the microscopic images of stained adjacent cross sections. The validity of the *m/z* based heat maps was assessed by additionally considering Na and K adducts as well as Cl isotope patterns (efavirenz and fluopyram) and the results of the LC-HRMS/MS analysis. GraphPad Prism 9 (GraphPad Software, Inc.) was used for LC-HRMS/MS data visualization.

3. Results and discussion

3.1. Experimental conditions

The mortality of exposed gammarids was < 7.5 % and thus no significant influence of the exposure mixture on gammarid physiology and toxicokinetics would be expected. Furthermore, this mortality is lower than the in OECD 305 (OECD, 2012) set threshold of 20 %. Over the time course of the exposure, the medium concentrations of the parent compounds deviated less than 10 % from the nominal exposure concentration (SI A5). No contaminants were detected in the control samples of medium and gammarids.

3.2. Contaminant concentration and distribution assessed by LC-HRMS/MS

The total internal concentrations of cyprodinil (23.8 ± 1.8 μmol kg^{-1}), fluopyram (8.2 ± 0.9 μmol kg^{-1}) and terbutryn (43.5 ± 6.9 μmol kg^{-1}) determined in the whole body extracts were in the predicted range based on bioconcentration factors after 24 h of exposure ($BCF_{24\ h}$, defined as the ratio of tissue and medium concentration after 24 h of exposure) in previous bioconcentration experiments (SI A6, Raths et al., 2023c). However, the internal concentrations of carbamazepine (23.7 ± 1.8 μmol kg^{-1}) and citalopram (35.3 ± 4.9 μmol kg^{-1}) were about two times lower than expected, indicating a concentration effect on toxicokinetics in gammarids. The bioconcentration potential of efavirenz (69.5 ± 5.1 μmol kg^{-1}) was for the first time assessed in gammarids resulting in a $BCF_{24\ h}$ of 217 ± 35 L kg^{-1}.

A total of 19 BTPs was identified using reference standards (level 1; Schymanski et al., 2014) or MS/MS spectra reported in literature (level 2a, Table S7, SI A3). Eight of these BTPs were found in concentrations ≥ 5 % of the parent concentration and were considered for the following data evaluation. The highest proportion of BTP compared to the parent compound in the total tissue was found for CIT_M311 (N-desmethyl citalopram) with 23 ± 3 % and TER_M315b with 12 ± 5 %.

A representative overview of contaminant concentrations in the

dissected compartments is presented in Fig. 2. Similarly across all parent compounds, the highest absolute concentrations were found in the gills, followed by the intestinal system with approximately one order of magnitude higher concentrations compared to the total tissue concentrations. Parent concentrations in the cephalon and remaining tissue were in a similar range to each other but tend to be higher in the cephalon. The highest concentrations of BTPs from cyprodinil and terbutryn were found in the intestinal system followed by the gills. This trend was reversed for citalopram and carbamazepine. BTP concentrations of fluopyram and efavirenz were all < 5 % of the parent concentrations and thus not quantified (SI A7).

The high concentrations found in the gills may be explained by the uptake route of the exposed contaminants. The main contact surface with the contaminated test medium are the gills. Thus, diffusion of contaminants into the organisms takes place largely at the gills, whereas diffusion through the cuticle or exoskeleton is possibly smaller due to lower permeability. Also for heavy metals the highest tissue specific concentrations in gammarids have been reported in the gill tissue (Gestin et al., 2022, 2021). The high concentrations of BTPs in gill tissue may be mostly a consequence of the high parent concentrations and proportional biotransformation. Biotransformation activity was reported for gill cell lines of fish, but at lower rates than in the liver or intestine (Gomez et al., 2010; Leguen et al., 2000; Stadnicka-Michalak et al., 2018). Such biotransformation capability of gill tissue may also apply for amphipods.

The high concentrations of parent contaminants and their BTPs in the intestinal system were expected and are in line with observations made by radio-imaging (Arts et al., 1995; Nyman et al., 2014; Raths et al., 2020). Because no food was available for exposed gammarids, distribution was caused by partitioning of contaminats taken up from the medium. The partitioning may be driven by passive diffusion towards the higher lipid content in the intestinal tissue, but possibly also by (active) transport, i.e. by ATP-binding cassette (ABC) transporters (Jeong et al., 2017), towards the sites of biotransformation or excretion. An effect of pH on the parent distribution pattern seems unlikely as the intestinal pH of *G. pulex* was reported to be in the range of 5.6 (Monk, 1977) which would have no or a negligible effect on the speciation of the test contaminants (pk_a provided in Table S1).

The intestinal system, especially the hepatopancreas, of crustaceans is known to contain high amount of biotransformation enzymes, such as CYP-450 (James, 1989), which explains the high BTPs content in this compartment. Furthermore, the gut microbiome may contribute to the biotransformation, but little is known about its actual contribution to biotransformation processes (Adamovsky et al., 2018). BTPs reached concentrations from 23 % (CIT_M311) up to 60 % (TER_M315b) of the parent compound in the intestine. This BTP/parent ratio was generally much lower and similar across the other compartments (gills, cephalon, and remaining tissue; SI A8). This is a clear indication that the intestinal system is the main site of biotransformation in *G. pulex*.

The identified BTPs were mostly Phase I BTPs created by dealkylation, hydroxylation, and oxidation. Such reactions are commonly catalyzed by enzymes of the CYP-450 family, flavin-containing monooxygenases (FMOs) or monoamine oxidases (MAO) and have been reported in gammarids before (Jeon et al., 2013; Rösch et al., 2017, 2016). Furthermore, glutathione conjugates followed by subsequent reactions to form cysteine conjugates (Phase II BTPs) were found for terbutryn. This transformation process may involve glutathione S-transferases (GSTs), carboxyl peptidases and glutamyl peptidases (Jeon et al., 2013).

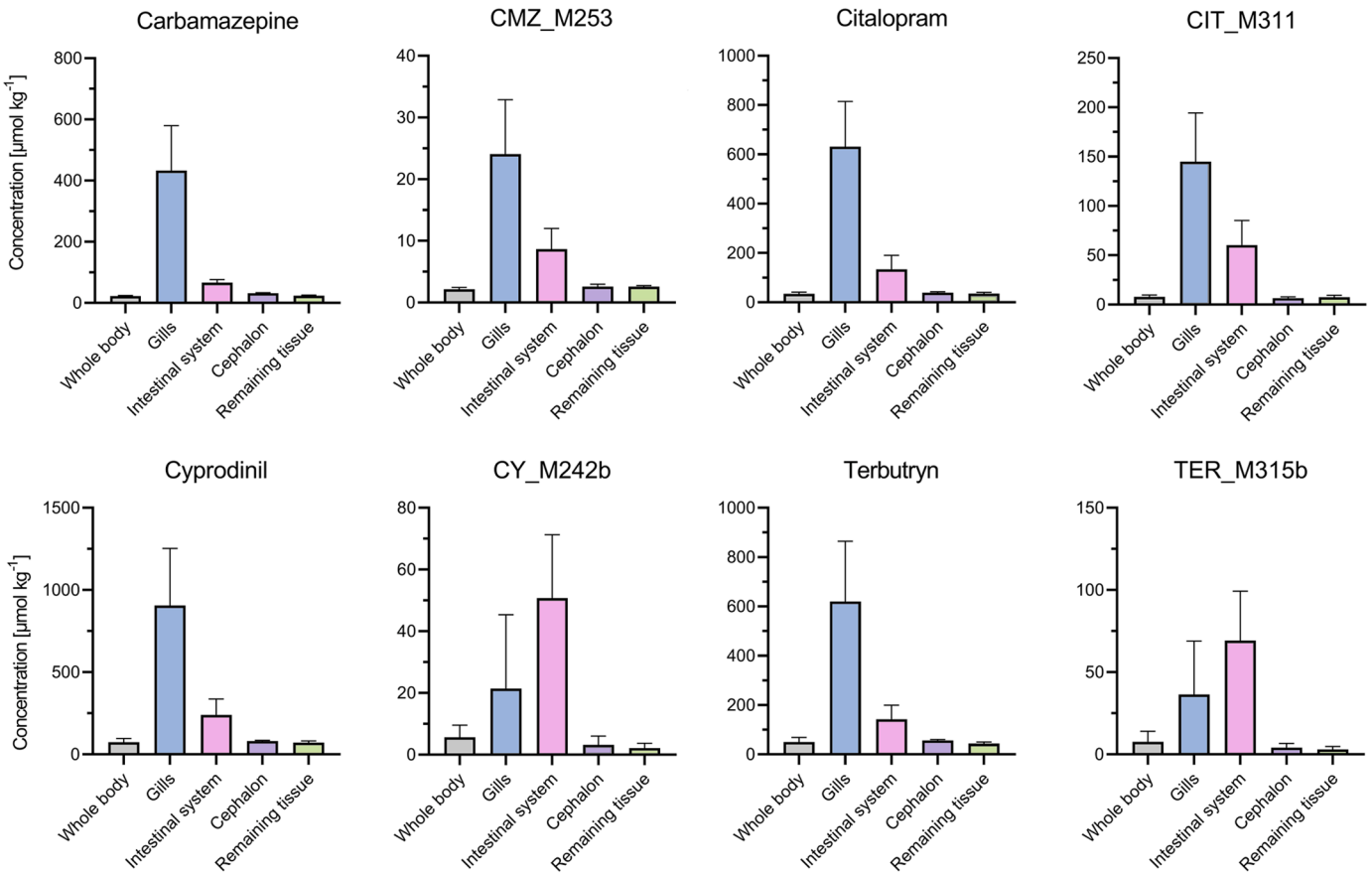

Fig. 2. Contaminant concentrations in the dissected compartments gammarids. Whole body = tissue concentration from whole body homogenate extracts. Please note the different y-axis scales. Single BTPs are shown as representatives for other BTPs with a similar distribution. Graphics for the other compounds, including efavirenz and fluopyram, are provided in SI A7.

The relative contribution of different compartments to the total body burden is presented in Fig. 3. Despite the high absolute parent concentrations in the gills and intestinal system, the contribution of these compartments to the total tissue concentration remained relatively low due to the low contributions of these compartments to the total body weight (0.15 ± 0.04 % for gills and 5.0 ± 0.8 % for the intestinal system). For the BTPs however, the contribution of the intestinal system showed a strong over-proportional contribution compared to the weight of this fractions and accounted for up to 56 ± 18 % (CY_M242b) of the total body burden. Apart from the strong biotransformation activity in the intestinal system, this may also indicate a low reallocation rate of BTPs from the intestinal system into surrounding tissue. The contribution of the intestinal system to the total body burden of BTPs of the psychoactive drugs carbamazepine and citalopram was lower than for the pesticides cyprodinil and terbutryn, but still much higher than its weight contribution.

3.3. Spatial contaminant distribution assessed by mass spectrometry imaging

Adjacent sagittal cryosections of gammarids were successfully created and analyzed by both MSI methods in a reproducible manner (Fig. 4). Muscular tissue, the ventral nerve, exoskeleton and intestinal system (including the hepatopancreas, confirmed by biomarkers in MSI) could be distinguished within the stained sections whereas gills and in some instances the eyes lay outside the sectioned area and the hemolymph system could not be distinguished. Membrane lipids could be successfully employed as biomarkers for general orientation in the tissue (i.e., phosphatidylcholine PC(34:1)) as well as specifically identify the ventral nerve (PC(38:4)) and hepatopancreas (*m/z* 666.3940 and 680.4100 according to Fu et al., 2021). The hepatopancreas biomarkers were only detected using MALDI-HRMS.

Four out of six parent compounds (carbamazepine, citalopram, cyprodinil, terbutryn) could be detected using MALDI but all six by using DESI (Table 2). All parent contaminants were detected across the whole sample but with highest intensities in the intestinal system (i.e., hepatopancreas, stomach), similar to the LC-HRMS/MS analysis of dissected gammarid compartments. Intensities were, in correspondence with the tissue concentrations, lower for carbamazepine, detected as potassium adduct $[M + K]^+$, efavirenz and fluopyram, which were best detected as potassium sodium adducts $[M+Na]^+$ in DESI. Most BTPs that were quantified by LC-HRMS/MS could also be detected using MSI. All detected BTPs followed a similar tissue distribution with highest intensities in the hepatopancreas area for both ionization techniques. These results are also in line with the observations by LC-HRMS/MS. CMZ_M253 was not detected, probably due to the low tissue concentration. TER_M214 and TER_M258a could not be detected sufficiently by DESI due to a background contamination of the exact same *m/z*, which was found also outside of the gammarid tissue and in the controls (SI A10). However, the relative intensity was much higher in the gammarid tissue for exposed gammarids than in the controls. The contamination was not known as a typical DESI contaminant and may originate from small organic compounds in the cryotape applied for keeping section integrity. The result was surprising as contaminants in the low *m/z* are generally more common for MALDI, caused by matrix ions (Calvano et al., 2018; Qiao and Lissel, 2021).

Surprisingly the spatial distribution of the psychoactive drug citalopram did not differ from the distribution of the other contaminants. It has been reported earlier that elevated citalopram concentrations were found in the nervous tissue of dissected fish (Grabicova et al., 2014; Schultz et al., 2010). Furthermore, MALDI-MSI of citalopram in fish found the highest intensities in the area of the spinal cord (Davis et al., 2020). Thus, similar observations would have been expected for gammarids. This assumption was also supported by the suggestion of an active uptake pathway of citalopram into amphipod nervous tissue (Raths et al., 2023c) which may be temperature dependent and saturable similar as reported for mammals (Rochat et al., 1999). One possible explanation may be the concentration dependence (saturation) of this uptake pathway. The $BCF_{24\,h}$ of citalopram was more than two times lower than reported for lower exposure concentrations (50 µg L^{-1}) (Raths et al., 2023c) which may indicate that active uptake has already been over-saturated at the tested concentration and the imaged proportion of citalopram might have been mostly distributed by passive diffusion.

3.4. Comparison of the analytical methods

The comparison of MALDI- and DESI-HRMS imaging (Table 2) indicated that both methods were suitable for the analysis of organic contaminants and their BTPs in gammarid tissue. In combining the two methods, additional confidence could be obtained by (a) using biomarkers detected by only one of the methods and by (b) compensating

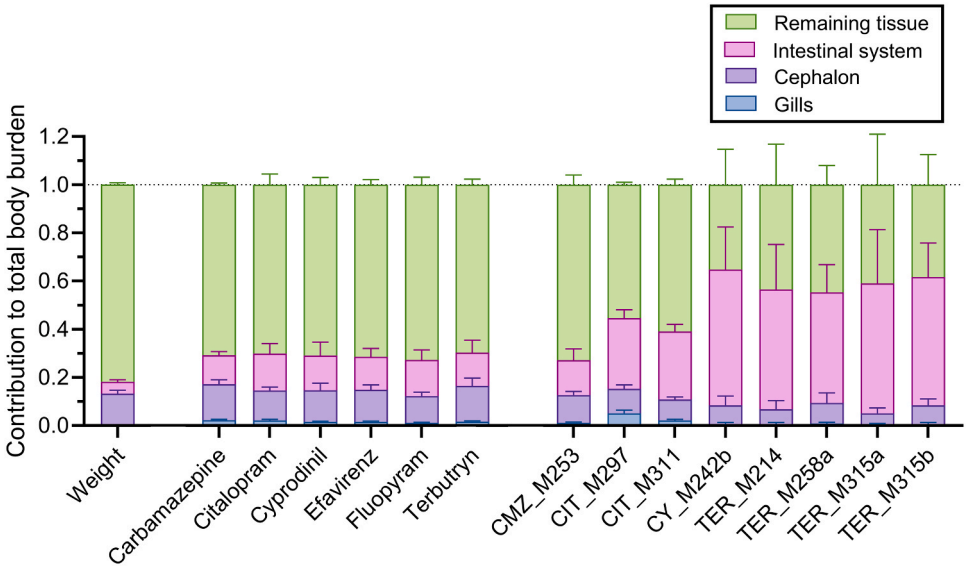

Fig. 3. Relative contribution of the dissected compartments to the whole body weight (left), total parent body burden (middle group) and body burden of their BTPs (right group).

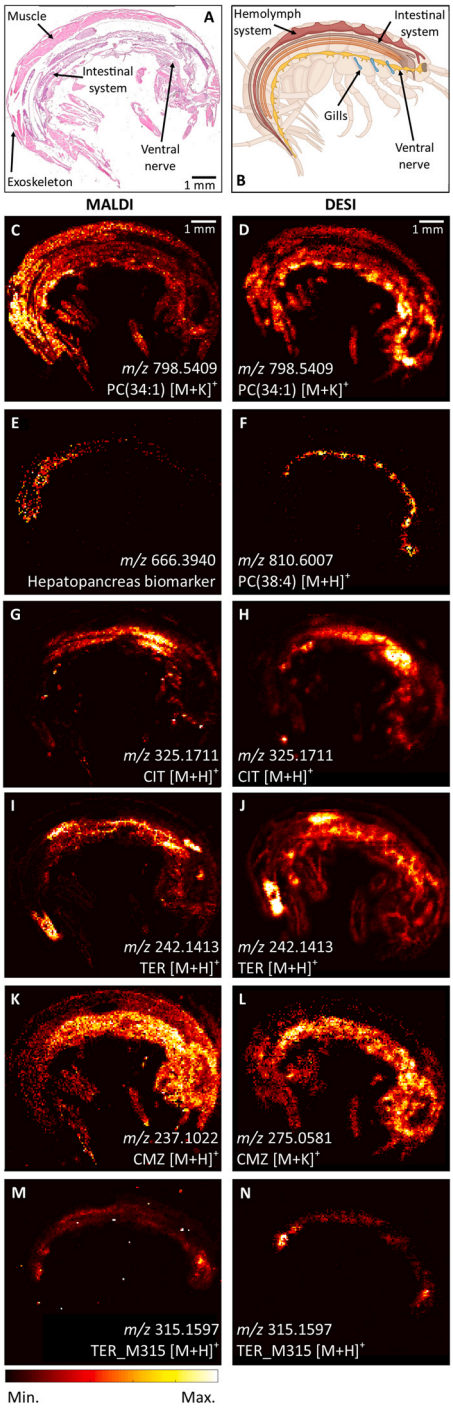

Fig. 4. (A) Stained sagittal cryosection. (B) Illustration of different organ compartments in *G. pulex*. Images from MALDI-HRMS on the left and DESI-HRMS on the right side. (C + D) Phosphatidylcholine PC(34:1) for orientation in the MS-images. (E) *m/z* 666.3940 = biomarker for the hepatopancreas (analogous image for *m/z* 680.4100) (Fu et al., 2021), (F) PC(38:4) as biomarker for the ventral nerve (analogous image to the same mass in MALDI). (G + H) CIT = citalopram, (I + J) TER = terbutryn (analogous image to cyprodinil), (K + L) CMZ = carbamazepine (analogous images for fluopyram and efavirenz $[M + Na]^+$), (M + N) TER_M315 (no distinction between isomers a and b possible in MSI) representative for all detected BTPs. The pixel size is 60 μm. Replicates and remaining compounds are presented in SI A9.

for artefacts present in one of the methods. MALDI appeared to be more sensitive for the hepatopancreas biomarker and for some BTPs, because of mass interferences in DESI mass spectra. DESI however was able to detect all six parent compounds whereas only four were detected using MALDI.

The utilization of adjacent cross sections appeared to be sufficient for generating comparable analyses. However, the subsequent analysis by DESI and MALDI on the same sample cross section has been performed elsewhere (Eberlin et al., 2011b) and may be a possible optimization method (i.e. for complementing biomarkers, including proteins). Such an approach would require a reduction of the destructiveness of the DESI method, which may be achieved by the use of different solvents (i.e. dimethylformamide) to preserve morphological features (Eberlin et al., 2011a) or lower solvent flow rate or gas pressure than what was applied here. In the present method, especially sections of the exoskeleton were very fragile and easily fell off after DESI analysis, which would prevent subsequent MALDI analysis and staining.

A pixel size of 60 μm was sufficient to localize contaminats on the level of whole organism cross sections, thus the higher special resolution of MALDI did not offer an advantage over DESI. However, it may be preferred to analyze more detailed spatial distribution patterns, such as within the brain of small organisms (Kirla et al., 2016; Phan et al., 2016) without causing oversampling. Such spatial resolution challenges for DESI may be overcome by the further development of nanospray DESI (nano-DESI; Lanekoff et al., 2012; Roach et al., 2010) or desorption electro-flow focusing ionization (DEFFI; Wu et al., 2022).

Both MSI methods had a lower sensitivity than the LC-HRMS/MS analysis. Furthermore, in MSI additional separation methods such as chromatography and fragmentation spectra (MS2) are often missing, making these methods prone to analytical artefacts. Thus, complementation of MSI analysis with additional confirmatory analysis, such as LC-HRMS/MS, is important.

When it comes to the analysis of target tissues, both analytical approaches may provide different capabilities of analyzing specific tissues. By using dissection and LC-HRMS/MS compartments such as the gills or antenna (here sampled as part of the cephalon) may be analyzed that are difficult to be caught on a whole body cryosection. Furthermore, samples of the circular system (hemolymph) may be taken separately (Vannuci-Silva et al., 2018). MSI techniques, however, allow to assess the spatial distribution in compartments that cannot be dissected, such as the exoskeleton and muscular tissue, the ventral nerve or microstructures in the brain. The present results demonstrated that DESI may be preferred as a more sensitive MSI method for small organic compounds, but MALDI may be used for more specific research questions (i.e. such that require a higher spatial resolution).

3.5. MSI application in environmental sciences

Despite a large potential for localizing environmental contaminants and elucidating toxicodynamic and toxicokinetic processes, MSI has only found its way into environmental sciences in the recent years and reports are still scarce (Maloof et al., 2020; Yang et al., 2020). This is mostly due to one major drawback of using MSI in environmental sciences, which is the relatively low sensitivity and thus high concentrations required for sufficient imaging. The exposure concentrations applied in the present study (100 μg L^{-1} to mg L^{-1} range) were several orders of magnitude higher than typically observed in the environment (ng L^{-1} up to low μg L^{-1} range; Lauper et al., 2021; Munz et al., 2018). Internal concentrations were in the μg g^{-1} range, whereas they are in the ng g^{-1} range in the environment. Such unrealistically high exposure concentrations may mask receptor binding (i.e. such as for neonicotinoids; Raths et al., 2023a) or active transport mechanism (speculated for citalopram; Raths et al., 2023c and the present study) that can reach saturation. Furthermore, compounds with higher toxicity cannot be studied using MSI, which was also a limitation in this study. The development and application of more efficient ionization methods is the

Table 2
Overview of the analyzed compounds and compatibility with the different analytical methods. *m/z* of sodium (^{Na}) and Potassium (^{K}) adducts $[M + Na]^+$ and $[M + K]^+$, respectively, are provided for compounds that were imaged using this mass. [a] = adducts undefined (Fu et al., 2021). X[b] = summarizes all BTPs with this mass in MSI, as MSI techniques did not allow for a chromatographic separation. Interference = detectable but interference with background masses (SI A10). Most BTPs that were not quantified by LC-HRMS/MS (< 5 % parent concentration, Table S7 & S8) were not found by either MSI method.

Compound	*m/z* $[M + H]^+$	*m/z* $[M + Na/K]^+$	LC-HRMS/MS	DESI-HRMS	MALDI-HRMS
Parents					
Carbamazepine (CMZ)	237.1022	275.0581^{K}	yes	yes^{K}	yes
Citalopram (CIT)	325.1710		yes	yes	yes
Cyprodinil (CY)	226.1338		yes	yes	yes
Efavirenz	316.0346	338.0166^{Na}	yes	yes^{Na}	no
Fluopyram	397.0536	419.0356^{Na}	yes	yes^{Na}	no
Terbutryn (TER)	242.1433		yes	yes	yes
Biomarkers					
Nervous system PC(38:4)	810.6007		n.a.	yes^{K}	yes^{K}
Hepatopancreas BM1[a]	666.3940[a]		n.a.	no	yes
Hepatopancreas BM2[a]	680.4100[a]		n.a.	no	yes
BTPs					
CMZ_M253	253.0971		yes	no	no
CIT_M297	297.1398		yes	yes	yes
CIT_M311	311.1554		yes	yes	yes
CY_M242x[b]	242.1288		yes	yes	yes
TER_M214	214.1121		yes	interference	yes
TER_M258x[b]	258.1383		yes	interference	yes
TER_M315x[b]	315.1597		yes	yes	yes

main challenge for the analysis of samples with environmental relevant concentrations. Potential technological approaches that may close this analytical gap for MALDI-MSI are the application of the recently developed MALDI-2 technology (Barré et al., 2019; Niehaus et al., 2019) that uses laser-induced post-ionization of the initial MALDI plume with a secondary laser beam, and/or the use of more efficient matrices (Calvano et al., 2018; Qiao and Lissel, 2021) including nano particle enhanced matrices (Ma et al., 2022; Wu et al., 2020). The described approaches were particularly developed to enhance the ionization efficiency of small molecules, such as pesticides and pharmaceuticals, with increasing intensities by up to multiple orders of magnitude. However, these enhancements are generally compound dependent. The sensitivity of DESI may be enhanced by employing desorption electro-flow focusing ionization (DEFFI), which generates a more focused jet than conventional DESI (Wu et al., 2022) resulting in increased intensities by orders of magnitude for biological samples. After these analytical improvements, experiments with environmental concentrations should be carried out in the future.

Although the detection of small organic molecules in environmental samples remains challenging, applications of MSI beyond the localization of contaminants may be applied. Such investigations include effects on the physiology of exposed organisms by integrated stress assessment using lipidomic and proteomic analysis. So far, some preliminary investigations have been carried out for zebrafish (Liu et al., 2020; Stutts et al., 2020) and crustaceans (Fu et al., 2021; Smith et al., 2022; Zhang et al., 2015). Other than organic contaminants, lipids and proteins are show higher sensitivities in MSI and are therefore less affected by sensitivity issues, which makes these approaches a promising alternative.

4. Conclusion

The applied LC-MS and MSI methods were suitable for the analysis of the spatial distribution of organic contaminants and their BTPs in the tissue of the aquatic invertebrate *G. pulex*. Gammarids could be successfully dissected into different compartments (i.e., gills, intestinal system) to be extracted separately. However, some tissue types such as the nervous system and muscular tissue were not dissectible. LC-HRMS/MS of dissected gammarid tissues provided the highest sensitivity and confidence in compound (i.e., BTP) identification. Reproducible adjacent cryosections of gammarids for MSI could be created using an adhesive cryo-tape. Following DESI-HRMSI was generally more sensitive than MALDI-HRMSI but suffered from some mass interferences, possibly originating from the cryo-tape. Additional biomarkers (i.e., for the hepatopancreas) were detected using MALDI. The present results demonstrate the complementary applications and benefits of the different analysis methods. One drawback of this study were the unrealistically high exposure concentrations that had to be applied in order to allow MSI. Thus, one of the main challenges to overcome for the establishment of MSI in environmental sciences is the low sensitivity for small molecules such as organic contaminants. Promising technological solutions to enhance ionization efficiency such as MALDI-2 and DEFFI are currently being developed and tested and potentially allow assessments at environmental relevant exposure concentrations.

CRediT authorship contribution statement

Johannes Raths: Conceptualization, Data curation, Investigation, Formal analysis, Methodology, Visualization, Writing – original draft. **Fernanda Endringer Pinto:** Methodology, Supervision. **Christian Janfelt:** Supervision, Writing – review & editing. **Juliane Hollender:** Conceptualization, Funding acquisition, Supervision, Writing – review & editing.

Declaration of Competing Interest

The authors declare that they have no known competing financial interests or personal relationships that could have appeared to influence the work reported in this paper.

Data Availability

ImzML files are uploaded to the metaspace database and are openly available at https://metaspace2020.eu/project/raths-2023. Other data will be made available on request.

Acknowledgements

We acknowledge financial support of the Swiss National Science Foundation (200020_184878). We thank Marcus Lorensen (Copenhagen University), Susanne Ulbrich and Anna-Katharina Hankele (ETH Zürich, AgroVet-Strickhof) for helpful discussions and use of their facilities for cryosectioning, respectively. We thank Syngenta Group Co., Ltd. for the provision of reference standards. Graphics were partially created using

https://biorender.com.

Supporting information

Provided are SI A (main SI section) and the excel sheet SI B (holds measured concentrations and explanation of metaspace file names). ImzML files are uploaded to the metaspace database and are openly available at https://metaspace2020.eu/project/raths-2023.

Appendix A. Supporting information

Supplementary data associated with this article can be found in the online version at doi:10.1016/j.ecoenv.2023.115468.

References

Adamovsky, O., Buerger, A.N., Wormington, A.M., Ector, N., Griffitt, R.J., Bisesi Jr, J.H., Martyniuk, C.J., 2018. The gut microbiome and aquatic toxicology: an emerging concept for environmental health. Environ. Toxicol. Chem. 37, 2758–2775. https://doi.org/10.1002/etc.4249.

Arts, M.T., Ferguson, M.E., Glozier, N.E., Robarts, R.D., Donald, D.B., 1995. Spatial and temporal variability in lipid dynamics of common amphipods: assessing the potential for uptake of lipophilic contaminants. Ecotoxicology 4, 91–113. https://doi.org/10.1007/BF00122171.

Ashauer, R., Hintermeister, A., O'Connor, I., Elumelu, M., Hollender, J., Escher, B.I., 2012. Significance of xenobiotic metabolism for bioaccumulation kinetics of organic chemicals in *Gammarus pulex*. Environ. Sci. Technol. 46, 3498–3508. https://doi.org/10.1021/es204611h.

Barré, F.P.Y., Paine, M.R.L., Flinders, B., Trevitt, A.J., Kelly, P.D., Ait-Belkacem, R., Garcia, J.P., Creemers, L.B., Stauber, J., Vreeken, R.J., Cillero-Pastor, B., Ellis, S.R., Heeren, R.M.A., 2019. Enhanced sensitivity using MALDI imaging coupled with laser postionization (MALDI-2) for pharmaceutical research. Anal. Chem. 91, 10840–10848. https://doi.org/10.1021/acs.analchem.9b02495.

Bokhart, M.T., Nazari, M., Garrard, K.P., Muddiman, D.C., 2018. MSiReader v1.0: evolving open-source mass spectrometry imaging software for targeted and untargeted analyses. J. Am. Soc. Mass Spectrom. 29, 8–16. https://doi.org/10.1007/s13361-017-1809-6.

Calvano, C.D., Monopoli, A., Cataldi, T.R.I., Palmisano, F., 2018. MALDI matrices for low molecular weight compounds: an endless story? Anal. Bioanal. Chem. 410, 4015–4038. https://doi.org/10.1007/s00216-018-1014-x.

Chaumot, A., Geffard, O., Armengaud, J., Maltby, L., 2015. Gammarids as reference species for freshwater monitoring. In: Aquatic Ecotoxicology. Elsevier, pp. 253–280.

Chughtai, K., Heeren, R.M.A., 2010. Mass spectrometric imaging for biomedical tissue analysis. Chem. Rev. 110, 3237–3277. https://doi.org/10.1021/cr100012c.

Davis, R.B., Hoang, J.A., Rizzo, S.M., Hassan, D., Potter, B.J., Tucker, K.R., 2020. Quantitation and localization of beta-blockers and SSRIs accumulation in fathead minnows by complementary mass spectrometry analyses. Sci. Total Environ. 741, 140331 https://doi.org/10.1016/j.scitotenv.2020.140331.

Dong, Y., Li, B., Aharoni, A., 2016. More than pictures: when MS imaging meets histology. Trends Plant Sci. 21, 686–698. https://doi.org/10.1016/j.tplants.2016.04.007.

Eberlin, L.S., Ferreira, C.R., Dill, A.L., Ifa, D.R., Cheng, L., Cooks, R.G., 2011a. Nondestructive, histologically compatible tissue imaging by desorption electrospray ionization mass spectrometry. ChemBioChem 12, 2129–2132. https://doi.org/10.1002/cbic.201100411.

Eberlin, L.S., Liu, X., Ferreira, C.R., Santagata, S., Agar, N.Y.R., Cooks, R.G., 2011b. Desorption electrospray ionization then MALDI mass spectrometry imaging of lipid and protein distributions in single tissue sections. Anal. Chem. 83, 8366–8371. https://doi.org/10.1021/ac202016x.

Escher, B.I., Hermens, J.L.M., 2002. Modes of action in ecotoxicology: their role in body burdens, species sensitivity, QSARs, and mixture effects. Environ. Sci. Technol. 36, 4201–4217. https://doi.org/10.1021/es015848h.

Fu, Q., Fedrizzi, D., Kosfeld, V., Schlechtriem, C., Ganz, V., Derrer, S., Rentsch, D., Hollender, J., 2020. Biotransformation changes bioaccumulation and toxicity of diclofenac in aquatic organisms. Environ. Sci. Technol. 54, 4400–4408. https://doi.org/10.1021/acs.est.9b07127.

Fu, T., Knittelfelder, O., Geffard, O., Clément, Y., Testet, E., Elie, N., Touboul, D., Abbaci, K., Shevchenko, A., Lemoine, J., Chaumot, A., Salvador, A., Degli-Esposti, D., Ayciriex, S., 2021. Shotgun lipidomics and mass spectrometry imaging unveil diversity and dynamics in *Gammarus fossarum* lipid composition. iScience 24, 102115. https://doi.org/10.1016/j.isci.2021.102115.

Gestin, O., Lacoue-Labarthe, T., Coquery, M., Delorme, N., Garnero, L., Dherret, L., Ciccia, T., Geffard, O., Lopes, C., 2021. One and multi-compartments toxico-kinetic modeling to understand metals' organotropism and fate in *Gammarus fossarum*. Environ. Int. 156, 106625 https://doi.org/10.1016/j.envint.2021.106625.

Gestin, O., Lopes, C., Delorme, N., Garnero, L., Geffard, O., Lacoue-Labarthe, T., 2022. Organ-specific accumulation of cadmium and zinc in *Gammarus fossarum* exposed to environmentally relevant metal concentrations. Environ. Pollut. 308, 119625 https://doi.org/10.1016/j.envpol.2022.119625.

Gomez, C.F., Constantine, L., Huggett, D.B., 2010. The influence of gill and liver metabolism on the predicted bioconcentration of three pharmaceuticals in fish. Chemosphere 81, 1189–1195. https://doi.org/10.1016/j.chemosphere.2010.09.043.

Grabicova, K., Lindberg, R.H., Östman, M., Grabic, R., Randak, T., Joakim Larsson, D.G., Fick, J., 2014. Tissue-specific bioconcentration of antidepressants in fish exposed to effluent from a municipal sewage treatment plant. Sci. Total Environ. 488–489, 46–50. https://doi.org/10.1016/j.scitotenv.2014.04.052.

Hume, K.D., Elwood, R.W., Dick, J.T.A., Morrison, J., 2005. Sexual dimorphism in amphipods: the role of male posterior gnathopods revealed in *Gammarus pulex*. Behav. Ecol. Sociobiol. 58, 264–269. https://doi.org/10.1007/s00265-005-0925-7.

James, M.O., 1989. Cytochrome P450 monooxygenases in crustaceans. Xenobiotica 19, 1063–1076. https://doi.org/10.3109/00498258909043162.

Jeon, J., Hollender, J., 2019. In vitro biotransformation of pharmaceuticals and pesticides by trout liver S9 in the presence and absence of carbamazepine. Ecotoxicol. Environ. Saf. 183, 109513 https://doi.org/10.1016/j.ecoenv.2019.109513.

Jeon, J., Kurth, D., Hollender, J., 2013. Biotransformation pathways of biocides and pharmaceuticals in freshwater crustaceans based on structure elucidation of metabolites using high resolution mass spectrometry. Chem. Res. Toxicol. 26, 313–324. https://doi.org/10.1021/tx300457f.

Jeong, C.-B., Kim, H.-S., Kang, H.-M., Lee, J.-S., 2017. ATP-binding cassette (ABC) proteins in aquatic invertebrates: evolutionary significance and application in marine ecotoxicology. Aquat. Toxicol. 185, 29–39. https://doi.org/10.1016/j.aquatox.2017.01.013.

Kampe, S., Schlechtriem, C., 2016. Bioaccumulation of hexachlorobenzene in the terrestrial isopod *Porcellio scaber*. Environ. Toxicol. Chem. 35, 2867–2873. https://doi.org/10.1002/etc.3473.

Kawamoto, T., Kawamoto, K., 2021. Preparation of thin frozen sections from nonfixed and undecalcified hard tissues using Kawamoto's Film Method (2020). In: Hilton, M. J. (Ed.), Skeletal Development and Repair: Methods and Protocols, Methods in Molecular Biology. Springer, US, New York, NY, pp. 259–281. https://doi.org/10.1007/978-1-0716-1028-2_15.

Kiefer, K., Müller, A., Singer, H., Hollender, J., 2019. New relevant pesticide transformation products in groundwater detected using target and suspect screening for agricultural and urban micropollutants with LC-HRMS. Water Res. 165, 114972 https://doi.org/10.1016/j.watres.2019.114972.

Kirla, K.T., Groh, K.J., Steuer, A.E., Poetzsch, M., Banote, R.K., Stadnicka-Michalak, J., Eggen, R.I., Schirmer, K., Kraemer, T., 2016. From the cover: zebrafish larvae are insensitive to stimulation by cocaine: importance of exposure route and toxicokinetics. Toxicol. Sci. 154, 183–193.

Kochmann, J., Laier, M., Klimpel, S., Wick, A., Kunkel, U., Oehlmann, J., Jourdan, J., 2023. Infection with acanthocephalans increases tolerance of *Gammarus roeselii* (Crustacea: Amphipoda) to pyrethroid insecticide deltamethrin. Environ. Sci. Pollut. Res. https://doi.org/10.1007/s11356-023-26193-0.

Lanekoff, I., Heath, B.S., Liyu, A., Thomas, M., Carson, J.P., Laskin, J., 2012. Automated platform for high-resolution tissue imaging using nanospray desorption electrospray ionization mass spectrometry. Anal. Chem. 84, 8351–8356. https://doi.org/10.1021/ac301909a.

Lauper, B.B., Anthamatten, E., Raths, J., Arlos, M., Hollender, J., 2021. Systematic underestimation of pesticide burden for invertebrates under field conditions: comparing the influence of dietary uptake and aquatic exposure dynamics. ACS Environ. Au 2 (2). https://doi.org/10.1021/acsenvironau.1c00023.

Leguen, I., Carlsson, C., Perdu-Durand, E., Prunet, P., Pärt, P., Cravedi, J.P., 2000. Xenobiotic and steroid biotransformation activities in rainbow trout gill epithelial cells in culture. Aquat. Toxicol. 48, 165–176. https://doi.org/10.1016/S0166-445X(99)00043-0.

Liu, W., Nie, H., Liang, D., Bai, Y., Liu, H., 2020. Phospholipid imaging of zebrafish exposed to fipronil using atmospheric pressure matrix-assisted laser desorption ionization mass spectrometry. Talanta 209, 120357. https://doi.org/10.1016/j.talanta.2019.120357.

Ma, C., Wang, X., Zhang, H., Liu, W., Wang, D., Liu, F., Lu, H., Huang, L., 2022. High-throughput screening and spatial profiling of low-mass pesticides using a novel Ti3C2 MXene nanowire (TMN) as MALDI MS matrix. Chemosphere 286, 131826. https://doi.org/10.1016/j.chemosphere.2021.131826.

Maloof, K.A., Reinders, A.N., Tucker, K.R., 2020. Applications of mass spectrometry imaging in the environmental sciences. Curr. Opin. Environ. Sci. Health Environ. Chem.: Innov. Approaches Instrum. Environ. Chem. 18, 54–62. https://doi.org/10.1016/j.coesh.2020.07.005.

Miller, T.H., McEneff, G.L., Stott, L.C., Owen, S.F., Bury, N.R., Barron, L.P., 2016. Assessing the reliability of uptake and elimination kinetics modelling approaches for estimating bioconcentration factors in the freshwater invertebrate, *Gammarus pulex*. Sci. Total Environ. 547, 396–404. https://doi.org/10.1016/j.scitotenv.2015.12.145.

Monk, D.C., 1977. The digestion of cellulose and other dietary components, and pH of the gut in the amphipod *Gammarus pulex* (L.). Freshw. Biol. 7, 431–440. https://doi.org/10.1111/j.1365-2427.1977.tb01692.x.

Mulisch, M., Welsch, U. (Eds.), 2015. Romeis - Mikroskopische Technik. Springer-Verlag.

Munz, N.A., Fu, Q., Stamm, C., Hollender, J., 2018. Internal concentrations in gammarids reveal increased risk of organic micropollutants in wastewater-impacted streams. Environ. Sci. Technol. 52, 10347–10358. https://doi.org/10.1021/acs.est.8b03632.

Mutlib, A.E., Gerson, R.J., Meunier, P.C., Haley, P.J., Chen, H., Gan, L.S., Davies, M.H., Gemzik, B., Christ, D.D., Krahn, D.F., Markwalder, J.A., Seitz, S.P., Robertson, R.T., Miwa, G.T., 2000. The species-dependent metabolism of efavirenz produces a nephrotoxic glutathione conjugate in rats. Toxicol. Appl. Pharm. 169, 102–113. https://doi.org/10.1006/taap.2000.9055.

Naylor, C., Maltby, L., Calow, P., 1989. Scope for growth in *Gammarus pulex*, a freshwater benthic detritivore. Hydrobiologia 188, 517–523. https://doi.org/10.1007/BF00027819.

Niehaus, M., Soltwisch, J., Belov, M.E., Dreisewerd, K., 2019. Transmission-mode MALDI-2 mass spectrometry imaging of cells and tissues at subcellular resolution. Nat. Methods 16, 925–931. https://doi.org/10.1038/s41592-019-0536-2.

Nyman, A.-M., Schirmer, K., Ashauer, R., 2014. Importance of toxicokinetics for interspecies variation in sensitivity to chemicals. Environ. Sci. Technol. 48, 5946–5954. https://doi.org/10.1021/es5005126.

OECD, 2012. Test No. 305: Bioaccumulation in Fish: Aqueous and Dietary Exposure. OECD Publishing, Paris.

Ohtsu, S., Yamaguchi, M., Nishiwaki, H., Fukusaki, E., Shimma, S., 2018. Development of a visualization method for imidacloprid in *Drosophila melanogaster* via imaging mass spectrometry. Anal. Sci. 34, 991–996. https://doi.org/10.2116/analsci.18SCP04.

Phan, N.T.N., Mohammadi, A.S., Dowlatshahi Pour, M., Ewing, A.G., 2016. Laser desorption ionization mass spectrometry imaging of Drosophila brain using matrix sublimation versus modification with nanoparticles. Anal. Chem. 88, 1734–1741. https://doi.org/10.1021/acs.analchem.5b03942.

Qiao, Z., Lissel, F., 2021. MALDI matrices for the analysis of low molecular weight compounds: rational design, challenges and perspectives. Chem. – Asian J. 16, 868–878. https://doi.org/10.1002/asia.202100044.

Raths, J., Kuehr, S., Schlechtriem, C., 2020. Bioconcentration, metabolism, and spatial distribution of 14C-labeled laurate in the freshwater amphipod *Hyalella azteca*. Environ. Toxicol. Chem. 39, 310–322. https://doi.org/10.1002/etc.4623.

Raths, J., Schinz, L., Mangold-Döring, A., Hollender, J., 2023a. Elimination resistance: characterizing multi-compartment toxicokinetics of the neonicotinoid thiacloprid in the amphipod *Gammarus pulex* using bioconcentration and receptor-binding assays. Environ. Sci. Technol. https://doi.org/10.1021/acs.est.3c01891.

Raths, J., Schnurr, J., Bundschuh, M., Pinto, F.E., Janfelt, C., Hollender, J., 2023b. Importance of dietary uptake for in situ bioaccumulation of systemic fungicides using *Gammarus pulex* as a model organism. Environ. Toxic. Chem. etc 5615. https://doi.org/10.1002/etc.5615.

Raths, J., Švara, V., Lauper, B., Fu, Q., Hollender, J., 2023c. Speed it up: how temperature drives toxicokinetics of organic contaminants in freshwater amphipods. Glob. Change Biol. 29, 1390–1406. https://doi.org/10.1111/gcb.16542.

Roach, P.J., Laskin, J., Laskin, A., 2010. Nanospray desorption electrospray ionization: an ambient method for liquid-extraction surface sampling in mass spectrometry. Analyst 135, 2233–2236. https://doi.org/10.1039/C0AN00312C.

Robichaud, G., Garrard, K.P., Barry, J.A., Muddiman, D.C., 2013. MSiReader: an open-source interface to view and analyze high resolving power MS imaging files on matlab platform. J. Am. Soc. Mass Spectrom. https://doi.org/10.1007/s13361-013-0607-z.

Rochat, B., Baumann, P., Audus, K.L., 1999. Transport mechanisms for the antidepressant citalopram in brain microvessel endothelium. Brain Res. 831, 229–236. https://doi.org/10.1016/S0006-8993(99)01461-4.

Rösch, A., Anliker, S., Hollender, J., 2016. How biotransformation influences toxicokinetics of azole fungicides in the aquatic invertebrate *Gammarus pulex*. Environ. Sci. Technol. 50, 7175–7188. https://doi.org/10.1021/acs.est.6b01301.

Rösch, A., Gottardi, M., Vignet, C., Cedergreen, N., Hollender, J., 2017. Mechanistic understanding of the synergistic potential of azole fungicides in the aquatic invertebrate *Gammarus pulex*. Environ. Sci. Technol. 51, 12784–12795. https://doi.org/10.1021/acs.est.7b03088.

Rubach, M.N., Ashauer, R., Maund, S.J., Baird, D.J., Brink, P.J.V. den, 2010. Toxicokinetic variation in 15 freshwater arthropod species exposed to the insecticide chlorpyrifos. Environ. Toxicol. Chem. 29, 2225–2234. https://doi.org/10.1002/etc.273.

Sangkuhl, K., Klein, T.E., Altman, R.B., 2011. PharmGKB summary: citalopram pharmacokinetics pathway. Pharmacogenet. Genom. 21, 769–772. https://doi.org/10.1097/FPC.0b013e328346063f.

Sapp, M., Ertunç, T., Bringmann, I., Schäffer, A., Schmidt, B., 2004. Characterization of the bound residues of the fungicide cyprodinil formed in plant cell suspension cultures of wheat. Pest Manag. Sci. 60, 65–74. https://doi.org/10.1002/ps.787.

Schlechtriem, C., Kampe, S., Bruckert, H.-J., Bischof, I., Ebersbach, I., Kosfeld, V., Kotthoff, M., Schäfers, C., L'Haridon, J., 2019. Bioconcentration studies with the freshwater amphipod *Hyalella azteca*: are the results predictive of bioconcentration in fish? Environ. Sci. Pollut. Res. 26, 1628–1641.

Schramm, T., Hester, Z., Klinkert, I., Both, J.-P., Heeren, R.M.A., Brunelle, A., Laprévote, O., Desbenoit, N., Robbe, M.-F., Stoeckli, M., Spengler, B., Römpp, A., 2012. imzML — a common data format for the flexible exchange and processing of mass spectrometry imaging data. J. Proteom. Spec. Issue.: Imaging Mass Spectrom.: A User's Guide A N. Tech. Biol. Biomed. Res. 75, 5106–5110. https://doi.org/10.1016/j.jprot.2012.07.026.

Schultz, M.M., Furlong, E.T., Kolpin, Dana W., Werner, S.L., Schoenfuss, H.L., Barber, L. B., Blazer, V.S., Norris, D.O., Vajda, A.M., 2010. Antidepressant pharmaceuticals in two U.S. effluent-impacted streams: occurrence and fate in water and sediment, and selective uptake in fish neural tissue. Environ. Sci. Technol. 44, 1918–1925. https://doi.org/10.1021/es9022706.

Schymanski, E.L., Jeon, J., Gulde, R., Fenner, K., Ruff, M., Singer, H.P., Hollender, J., 2014. Identifying small molecules via high resolution mass spectrometry: communicating confidence. Environ. Sci. Technol. 48, 2097–2098. https://doi.org/10.1021/es5002105.

Smith, M.J., Weber, R.J.M., Viant, M.R., 2022. Spatially mapping the baseline and bisphenol-A exposed *Daphnia magna* lipidome using desorption electrospray ionization-mass spectrometry. Metabolites 12, 33. https://doi.org/10.3390/metabo12010033.

Stadnicka-Michalak, J., Weiss, F.T., Fischer, M., Tanneberger, K., Schirmer, K., 2018. Biotransformation of benzo[a]pyrene by three rainbow trout (*Onchorhynchus mykiss*) cell lines and extrapolation to derive a fish bioconcentration factor. Environ. Sci. Technol. 52, 3091–3100. https://doi.org/10.1021/acs.est.7b04548.

Strohalm, M., Strohalm, J., Kaftan, F., Krásný, L., Volný, M., Novák, P., Ulbrich, K., Havlíček, V., 2011. Poly[N-(2-hydroxypropyl)methacrylamide]-based tissue-embedding medium compatible with MALDI mass spectrometry imaging experiments. Anal. Chem. 83, 5458–5462. https://doi.org/10.1021/ac2011679.

Stutts, W.L., Knuth, M.M., Ekelöf, M., Mahapatra, D., Kullman, S.W., Muddiman, D.C., 2020. Methods for cryosectioning and mass spectrometry imaging of whole-body zebrafish. J. Am. Soc. Mass Spectrom. 31, 768–772. https://doi.org/10.1021/jasms.9b00097.

Thunig, J., Hansen, S.H., Janfelt, C., 2011. Analysis of secondary plant metabolites by indirect desorption electrospray ionization imaging mass spectrometry. Anal. Chem. 83, 3256–3259. https://doi.org/10.1021/ac2004967.

Vannuci-Silva, M., da Silva, E. do N., Artal, M.C., Santos, A. dos, Silva, F., Umbuzeiro, G. de A., Cadore, S., 2018. GFAAS and ICP-MS determination of Ag and Cu in the haemolymph of a millimetric marine Crustacean (*Parhyale hawaiensis*) as a tool in ecotoxicology. At. Spectrosc. 39, 67–74. https://doi.org/10.46770/AS.2018.02.003.

Vargas-Pérez, M., Egea González, F.J., Garrido Frenich, A., 2020. Dissipation and residue determination of fluopyram and its metabolites in greenhouse crops. J. Sci. Food Agric. 100, 4826–4833. https://doi.org/10.1002/jsfa.10542.

Wang, Z., Walker, G.W., Muir, D.C.G., Nagatani-Yoshida, K., 2020. Toward a global understanding of chemical pollution: a first comprehensive analysis of national and regional chemical inventories. Environ. Sci. Technol. 54, 2575–2584. https://doi.org/10.1021/acs.est.9b06379.

Wu, V., Tillner, J., Jones, E., McKenzie, J.S., Gurung, D., Mroz, A., Poynter, L., Simon, D., Grau, C., Altafaj, X., Dumas, M.-E., Gilmore, I., Bunch, J., Takats, Z., 2022. High resolution ambient MS imaging of biological samples by desorption electro-flow focussing ionization. Anal. Chem. 94, 10035–10044. https://doi.org/10.1021/acs.analchem.2c00345.

Wu, X., Qin, R., Wu, H., Yao, G., Zhang, Y., Li, P., Xu, Y., Zhang, Z., Yin, Z., Xu, H., 2020. Nanoparticle-immersed paper imprinting mass spectrometry imaging reveals uptake and translocation mechanism of pesticides in plants. Nano Res. 13, 611–620. https://doi.org/10.1007/s12274-020-2700-5.

Yang, F.-Y., Chen, J.-H., Ruan, Q.-Q., Saqib, H.S.A., He, W.-Y., You, M.-S., 2020. Mass spectrometry imaging: an emerging technology for the analysis of metabolites in insects. Arch. Insect Biochem. Physiol. 103, e21643 https://doi.org/10.1002/arch.21643.

Zeumer, R., Hermsen, L., Kaegi, R., Kühr, S., Knopf, B., Schlechtriem, C., 2020. Bioavailability of silver from wastewater and planktonic food borne silver nanoparticles in the rainbow trout *Oncorhynchus mykiss*. Sci. Total Environ. 706, 135695 https://doi.org/10.1016/j.scitotenv.2019.135695.

Zhang, Y., Buchberger, A., Muthuvel, G., Li, L., 2015. Expression and distribution of neuropeptides in the nervous system of the crab *Carcinus maenas* and their roles in environmental stress. Proteomics 15, 3969–3979. https://doi.org/10.1002/pmic.201500256.

Zhang, Y., Chen, D., Du, M., Ma, L., Li, P., Qin, R., Yang, J., Yin, Z., Wu, X., Xu, H., 2021. Insights into the degradation and toxicity difference mechanism of neonicotinoid pesticides in honeybees by mass spectrometry imaging. Sci. Total Environ. 774, 145170 https://doi.org/10.1016/j.scitotenv.2021.145170.